Multiphoton Ionization Mass Spectrometric Studies of a Bichromophoric Molecule: 3-Phenyl-1-(*N*,*N*-dimethylamino)propane

D. A. Lichtin,† D. W. Squire, M. A. Winnik,* and R. B. Bernstein‡

Contribution from the Department of Chemistry, Columbia University, New York, New York 10027, and Lash Miller Laboratories, Department of Chemistry and Erindale College, University of Toronto, Toronto, Ontario, M5S 1A1 Canada.
Received June 30, 1982

Abstract: Multiphoton ionization (MPI) fragmentation studies of the bichromophoric molecule 3-phenyl-1-(*N*,*N*-dimethylamino)propane (P3NM) have been conducted in the wavelength regions 415–530 and 372–377 nm. These correspond respectively to the two-photon L_b and 3p Rydberg transitions of the phenyl group. Nevertheless, the overall fragmentation behavior of the molecule is dominated by the strong tertiary amine MPI process which has a broad, unstructured wavelength dependence. However, an increase in total ion yield from P3NM is observed at wavelengths in the two-photon resonance with the L_b state of the phenyl group, indicating independent (i.e., additive) excitation via both chromophores. Comparison of the behavior of P3NM with that of trimethylamine and toluene provides evidence for rapid, intramolecular energy transfer out of each chromophore in P3NM before fragmentation; i.e., energy redistributes out of both chromophores. The energetics of the fragmentation process, as well as possible reasons for an observed enhancement in ionization yield for P3NM (compared with that of trimethylamine and toluene) in the near-UV, are discussed.

Introduction

The processes of multiphoton ionization (MPI) fragmentation have been the subject of many recent theoretical and experimental studies.[1-17] For certain molecules, a statistical model successfully reproduces experimental results; for other molecules, dynamic processes must be taken into account. Examples of these two extremes are aromatics and uncaged tertiary amines.

The MPI two-photon resonant excitation spectra of simple aromatic molecules are rich in fine structure.[1-3] The initial, rate-limiting, simultaneous two-photon absorption is followed by subsequent photon absorption, increasing the energy of the neutral. Once the ionization energy is reached, prompt ejection of a low-energy electron occurs.[4,5] Fragmentation occurs by excitation up the "ionic ladder".[6] Because the simple aromatic molecular ions $M^{+\cdot}$ tend to be strong absorbers at frequencies from 370 to 530 nm, successive fragmentation by continued absorption is often observed during the ca. 5-ns laser pulse. For example, MPI excitation of toluene and of ethylbenzene, which have similar MPI signal strength, yields only traces of $M^{+\cdot}$ and $C_7H_7^+$ (m/z 91), both of which absorb at these wavelengths,[18] but yields high intensities of $C_3H_3^+$ (m/z 39) and $C^{+\cdot}$ (m/z 12).[19]

The MPI two-photon resonant excitation spectra of acyclic tertiary amines are broad and structureless,[7] resembling the one-photon spectra of these molecules. Their MPI fragmentation patterns are relatively simple. This is attributed to small cross sections for one-photon excitation in amine ions which restricts ion photodissociation. Only at very high laser powers (or in the case of caged tertiary amines) does one observe a significant amount of further fragmentation of $M^{+\cdot}$ and its primary daughter ions.[7] For example, MPI excitation of trimethylamine (TMA) over the range λ 370–530 nm leads to formation only of $M^{+\cdot}$ and $[M-H]^+$ (m/z 58). At shorter wavelengths (e.g., 355 nm) where $M^{+\cdot}$ absorbs, further fragmentation occurs to generate ions at masses 44 and 42, as well as a cluster of ions at masses 27–31.

Thus far most MPI studies have been confined to monochromophoric compounds. It is of interest to consider the MPI process for a molecule containing both a phenyl group and a tertiary amine. Presumably, wavelengths could be found suitable for enhanced excitation of either chromophoric group. Consequently, such a molecule facilitates the investigation of energy redistribution in large molecules by examining the wavelength and power de-

Scheme I

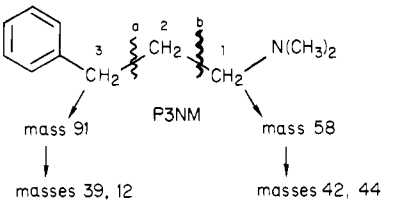

† Current Address: Chemistry Division, Naval Research Laboratory, Washington, D.C. 20375.

‡ Current Address: Occidental Research Corp., Irvine, CA 92713.

* To whom correspondence should be addressed at Lash Miller Laboratories.

(1) (a) D. A. Lichtin, S. Datta-Ghosh, K. R. Newton, and R. B. Bernstein, *Chem. Phys. Lett.*, **75**, 214 (1980); (b) K. R. Newton, D. A. Lichtin, and R. B. Bernstein, *J. Phys. Chem.*, **85**, 15 (1981); (c) D. A. Lichtin, R. B. Bernstein, and V. Vaida, *J. Am. Chem. Soc.*, **104**, 1830 (1982).

(2) (a) K. R. Newton, Ph.D. Thesis, Columbia University, 1981; (b) K. R. Newton and R. B. Bernstein, *J. Phys. Chem.*, in press.

(3) G. O. Uneberg, P. A. Campo, and P. M. Johnson, *J. Chem. Phys.*, **73**, 1110 (1980).

(4) J. T. Meek, R. K. Jones, and J. P. Reilly, *J. Chem. Phys.*, **73**, 3503 (1980).

(5) (a) J. C. Miller and R. N. Compton, *J. Chem. Phys.*, **75**, 2020 (1981); (b) C. D. Cooper, A. D. Williamson, J. C. Miller, and R. N Compton, *ibid.*, **73**, 1527 (1980).

(6) U. Boesl, H. J. Neusser, and E. W. Schlag, *J. Chem. Phys.*, **72**, 4327 (1980).

(7) D. H. Parker, R. B. Bernstein, and D. A. Lichtin, *J. Chem. Phys.*, **75**, 2577 (1981), and references cited therein.

(8) (a) J. Silberstein and R. D. Levine, *Chem. Phys. Lett.*, **74**, 6 (1980); (b) *J. Chem. Phys.*, **75**, 5735 (1981), and references cited therein; (c) D. A. Lichtin, R. B. Bernstein, and K. R. Newton, *ibid.*, **75**, 5728 (1981).

(9) (a) F. Rebentrost, K. L. Kompa, and A. Ben-Shaul, *Chem. Phys. Lett.*, **77**, 394 (1981); (b) F. Rebentrost and A. Ben-Shaul, *J. Chem. Phys.*, **74**, 3255 (1981).

(10) (a) J. P. Reilly and K. L. Kompa, *J. Chem. Phys.*, **73**, 5468 (1980); (b) W. Dietz, H. J. Neusser, U. Boesl, E. W. Schlag, and S. H. Lin, *Chem. Phys.*, **66**, 105 (1982); (c) G. J. Fisanick, T. S. Eichelberger IV, B. A. Heath, and M. B. Robin, *J. Chem. Phys.*, **72**, 5571 (1980); (d) D. S. Zakheim and P. M. Johnson, *Chem. Phys.*, **46**, 263 (1980).

(11) (a) D. H. Parker and P. Avouris, *J. Chem. Phys.*, **71**, 1241 (1979); (b) *Chem. Phys. Lett.*, **53**, 78 (1978).

(12) (a) K. Krogh-Jespersen, R. P. Rava, and L. Goodman, *Chem. Phys.*, **44**, 295 (1979); (b) L. Goodman and R. P. Rava, *J. Chem. Phys.*, **74**, 4826 (1981).

(13) L. Zandee and R. B. Bernstein, *J. Chem. Phys.*, **71**, 1359 (1979).

(14) T. G. Dietz, M. A. Duncan, M. G. Liverman, and R. E. Smalley, *Chem. Phys. Lett.*, **70**, 246 (1980).

(15) (a) P. M. Johnson and C. E. Otis, *Annu. Rev. Phys. Chem.*, **32**, 139 (1982); (b) R. B. Bernstein, *J. Phys. Chem.*, **86**, 1178 (1982); (c) P. M. Johnson, *Acc. Chem. Res.*, **13**, 20 (1980).

0002-7863/83/1505-2109$01.50/0

pendence of their fragmentation patterns.

As mentioned above, a statistical approach[8,9] has proven helpful in explaining the main features of MPI fragmentation patterns of polyatomic molecules. Such a theory implies rapid energy equilibration in a bichromophoric molecule. This treatment makes no attempt to deal with specific, structurally sensitive factors and pathways to the continuum. (However, a number of kinetic models have dealt with this problem with some success.[9,10])

The bichromophore 3-phenyl-1-(*N,N*-dimethylamino)propane [$C_6H_5(CH_2)_3N(CH_3)_2$ (P3NM)] was chosen for the present study. This choice was governed by several factors. First, the one-photon UV absorption spectrum of P3NM is identical with the superposition of those of toluene and trimethylamine (TMA).[20] This observation suggests that there are no interactions between the amine and phenyl groups (separated by three methylene groups) in the ground electronic state of the molecule. Second, the amine and toluene chromophores have nearly isoenergetic lowest excited singlet states, with that of the aromatic ring estimated to be 500–1000 cm^{-1} lower in energy.[21] The latter factor encourages the expectation of energy redistribution. In addition, the MPI and electron ionization (EI) processes for each chromophore have previously been studied,[1,2,7] laying the ground work for interpreting experiments on P3NM. Finally, the ionization energy of the homologous compound $C_6H_5(CH_2)_2N(CH_3)_2$ (P2NM) has been measured (7.7 eV)[22] and is close to that of trimethylamine (7.8 eV).

One of the most attractive features of P3NM is that it possesses two "weak" bonds which might cleave upon MPI or EI excitation (see Scheme I). Ionization of alkylbenzenes causes bond a to rupture, leading to the formation of the benzyl cation $C_7H_7^+$ (m/z 91). Further fragmentation of this ion leads primarily to ions of mass 39 and mass 12. Fragments of masses 91 (weak because of further absorption), 39, and 12 would be anticipated for processes occurring owing to MPI excitation at the "phenyl end" of P3NM. Ionization of acyclic tertiary amines cleaves bond b with the ion of mass 58 expected to be predominant in the mass spectrum. Ions of mass 58 (and possibly 42 and 44) would be diagnostic for amine-centered fragmentation. While resonant excitation of the phenyl group might lead to selective cleavage of bond a and selective amine excitation might lead to selective cleavage of bond b, energy transfer within electronically excited P3NM or electron transfer within the molecular ion might lead to other effects.

The one-photon UV solution photochemistry and spectroscopy of P3NM has been studied in detail.[20] Below room temperature P3NM adopts conformations in which the phenyl and dimethylamino groups are separated and do not interact. After excitation of the molecule into its lowest singlet state, rapid conformational changes occur on the time scale of ca. 100 ps at room temperature, permitting the molecule to fold into the (gauche$^{\pm}$–gauche$^{\mp}$) exciplex state with the amine adjacent to the phenyl ring. Fluorescence in solution at temperatures above −30 °C occurs exclusively from the exciplex state. While the binding energy of the exciplex is unknown, it may be estimated to be 0.2 to 0.4 eV.[23] For isolated molecules in the vapor phase, fluorescence occurs only from the isolated chromophores.[23] Little or no exciplex emission is observed. Either the free molecules do not have sufficient time to surmount the 0.1 to 0.2 eV rotational barrier in order to form the exciplex, or the molecule is unable to dissipate its excess energy in the absence of a solvent bath. Nonetheless, exciplex emission in solution is symptomatic of the existence of charge-transfer states in P3NM which do not exist in toluene or TMA. The energies of these states should depend on the conformation of P3NM.

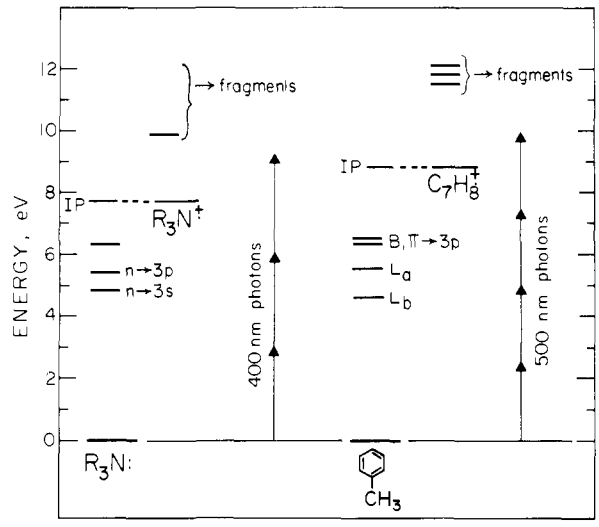

Figure 1. Energy level diagrams for the multiphoton ionization fragmentation of acyclic tertiary amines and toluene. States involved in two-photon resonance enhancement of these processes are shown. Also labeled are the ionization and appearance energies of these species, using the values for trimethylamine as typical for the former category. Arrows show photon energy at the indicated wavelengths.

The molecule P3NM can undergo rotations about four internal bonds. Only rotations about the C_1–C_2 or C_2–C_3 bonds (labeled b and a, respectively, in Scheme I) affect the separation of amine and phenyl groups. In the ground electronic state at room temperatures only the trans–trans (tt), trans–gauche (tg), and gauche$^{\pm}$–gauche$^{\pm}$ ($g^{\pm}g^{\pm}$) rotational conformations are energetically accessible.[20] In these conformations the end groups interact only weakly, not only in the ground state, but also in the lowest electronically excited singlet and the lowest triplet states. Charge-transfer (CT) states of the molecule do exist; however, little is known about them except that, when the molecule folds into the g^+g^- or g^-g^+ conformation, the lowest CT state (the exciplex state) becomes lower in energy than either locally excited singlet state.[20] This pair of conformations, which is strongly sterically destabilized in S_0, may also be favored in the molecular ion.

Figure 1 compares the energies of the lowest singlet excited states of tertiary amines and simple alkylbenzenes. Since acyclic tertiary amines have very broad and diffuse UV absorption and MPI spectra, there is some uncertainty in assigning (0,0) band energies. Corresponding caged amines which are electronically similar, but structurally rigid, have richly structured UV absorption/emission spectra[24] and MPI excitation spectra.[11] It is useful, therefore, to follow Halpern[24] in using 1-azabicyclo-[2.2.2]octane [ABCO, $N(CH_2CH_2)_3CH$] as an approximate model for identifying the onset of the low-energy transitions in TMA, TEA, and P3NM. As shown in Figure 1, the two lowest energy transitions in ABCO are the 3s and 3p Rydberg transitions.[24] The next lowest lying state, at 6.3 eV, is also a Rydberg state. The lowest energy transitions of monoalkylbenzenes are the L_a, L_b, and B bands,[12,25] as well as a ($\pi \rightarrow$ 3p) Rydberg transition.[16] These amine-centered Rydberg states and phenyl-centered valence and Rydberg states serve as resonant intermediate states for the REMPI process.[7,11,12]

(16) G. C. Nieman and S. D. Colson, *J. Chem. Phys.*, **68**, 5656 (1978).
(17) R. S. Pandolfi, D. A. Gobell, and M. A. El-Sayed, *J. Phys. Chem.*, **85**, 1779 (1981).
(18) (a) R. C. Dunbar, *J. Am. Chem. Soc.*, *95*, 472 (1973); (b) P. P. Dymerski, E. Fu, and R. C. Dunbar, *ibid.*, *96*, 4109 (1974).
(19) D. A. Lichtin, D. W. Squire, and R. B. Bernstein, unpublished results.
(20) M. Van der Auweraer, A. Gilbert, and F. C. De Schryver, *J. Am. Chem. Soc.*, **102**, 4007 (1980).
(21) Using 1-azabicyclo[2.2.2]octane (ABCO) as a model for unstrained tertiary amines, one finds the 0–0 band of the $S_1 \leftarrow S_0$ transition (3s ← n) at 39 080 cm^{-1} (255.9 nm, 4.85 eV) (ref 22). The 0–0 band of the $S_1 \leftarrow S_0$ transition (L_b) in toluene occurs at 37 500 cm^{-1} (266.7 nm, 4.65 eV) (ref 12a).
(22) Y. Loguinov, V. V. Takhistov, and L. P. Vatlina, *Org. Mass Spectrom.*, **16**, 239 (1981).
(23) M. A. Winnik, unpublished results.
(24) (a) A. M. Halpern, *J. Am. Chem. Soc.*, **96**, 7655 (1974); (b) A. M. Halpern, J. L. Roebber, and K. Weiss, *J. Chem. Phys.*, **49**, 1348 (1968); (c) A. M. Halpern, *Mol. Photochem.*, **5**, 517 (1973).
(25) J. B. Birks, "Photophysics of Aromatic Molecules", Wiley, New York, 1971.

Scheme II

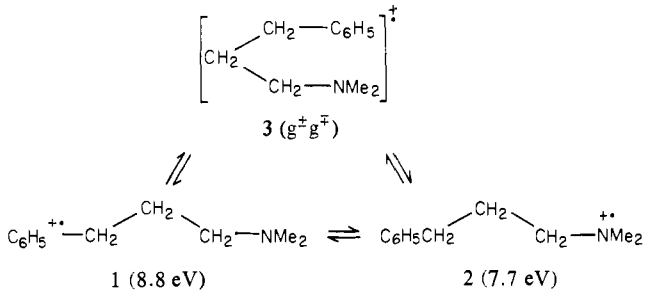

The gas-phase UV (one-photon) absorption spectrum of P3NM[20] in the 200–280-nm region resembles the superposition of the absorption spectra of toluene[12,25] and trimethylamine.[24] Thus, there is no prior evidence for low-lying charge-transfer (CT) states of substantial oscillator strength. The location of any such states in P3NM is unknown, although it seems reasonable that their energies will depend upon the molecular conformation.

It is assumed that the initial excitation in the MPI process will produce excited states localized on either the amine group or the phenyl ring. Following this excitation, energy transfer between localized states or crossing to CT states are processes possible in P3NM that cannot occur in toluene or TMA.

The ionization energies of toluene and ethylbenzene are 8.80 and 8.78 eV, respectively,[26] while those of trimethylamine and triethylamine are 7.80 and 7.50 eV, respectively.[26] In conformations where the end groups are nonadjacent, one would therefore anticipate the lowest ionization energy for P3NM to be in the range from 7.5 to 7.8 eV. The lowest ionization energy of P2NM [$C_6H_5CH_2CH_2NMe_2$] was recently reported to be 7.7 eV.[22] From all the available data one can reasonably interpret the molecular ion $M^{+\cdot}$ of P3NM as a mixture of the three structures of Scheme II.

Phenyl ionization produces ion **1**. Its charge is localized on the phenyl group, and $M^{+\cdot}$ in this form should have an absorption spectrum analogous to the toluene cation. Amine ionization produces ion **2** with the charge localized on the amine nitrogen. In this form $M^{+\cdot}$ should have the absorption spectrum typical of the TMA cation. This point is important because one of the distinguishing features of acyclic tertiary amine MPI behavior is that amine molecular ions appear to be transparent to one-photon excitation in the 370–530-nm region.[7] Aromatic ions absorb strongly in this region, and fragmentation occurs via excitation of these ions during the 5-ns laser pulse.

While the absorption characteristics and energy of the folded conformation **3** are unknown, it should be noted that this ion cannot be produced by vertical excitation since ground-state species in this conformation are negligibly populated.

The propriety of choosing TMA and toluene as model compounds for the fragmentation of P3NM can be questioned. Different molecules might be more appropriate to compensate for any effects of the alkyl chain on P3NM fragmentation. It has been demonstrated in acyclic tertiary amines that the breaking of the weakest bond on the carbon α to the nitrogen is the principal fragmentation step under MPI conditions.[7] Likewise, in the MPI fragmentation of toluene, *tert*-butylbenzene, and ethylbenzene, $C_7H_7^+$ has been a primary ionic product.[8c,19] The availability of extensive literature on the MPI behavior of TMA and toluene more than offsets the slight risk of an "alkyl chain effect" in P3NM.

Experimental Section

The major features of the laser time-of-flight mass spectrometer (LTOFMS) have been previously described.[1,2] Briefly, the output of a Nd:YAG pumped dye laser system (Quanta-Ray DCR-1/PDL-1) was focused into the ionization region of a time-of-flight mass spectrometer (CVC MA-2). The output from the mass spectrometer was processed through a waveform recorder (Biomation 6500) into a microcomputer (DEC MINC-11). Average power was measured with a volume or surface absorbing disk calorimeter (Scientech). The ca. 5-ns laser pulse was focused into the ionization region using a 0.25- or 0.50-m focal length fused silica spherical lens.

Table I. Observed Fragments from P3NM: 70-eV EI[a]

mass[d]	tentative assignments	rel intensity
$28^{R,B}$	CH_2N^+ or $C_2H_4^{+\cdot}$ (+ $N_2^{+\cdot}$)	2.6 ± 0.5
30^{R}	CH_4N^+ or $C_2H_6^{+\cdot}$	3.6
39	$C_3H_3^+$	3.5
41	$HCNCH_2^{+\cdot}$ or $C_3H_5^+$ or $C_2H_3N^{+\cdot}$	2.5
42	$C_2H_4N^{+\cdot}$	9.0
43	$C_2H_5N^+$	3.2
44	$C_2H_6N^+$	4.2
51	$C_4H_3^+$	2.8
57	$C_3H_7N\cdot$	3.3
58^{b}	$CH_2N(CH_3)_2^+$	100.0
$59^{R,I,B}$	$N(CH_3)_3^{+\cdot}$	9.6
65	$C_5H_5^+$	2.4
71	$C_4H_9N^{+\cdot}$	1.6
91^{c}	$C_7H_7^+$	6.7
163^{M}	$C_6H_5(CH_2)_3N(CH_3)_2^{+\cdot}$	12.0

[a] The 15 most intense peaks from mass spectrum of Figure 3a, 70 eV, 3.6×10^{-6} torr. [b] Cleavage of 1,2 bond, α to amino group. [c] Cleavage of 1,2 bond, α to phenyl group. [d] M = molecular ion, R = rearrangement product, I = isotopic species, B = background species.

The choice of lens was made to avoid saturation of the initial two-photon transition. Nonsaturation was indicated by a quadratic dependence of the total ion signal on laser power. This enabled comparison of separate molecules of greatly different signal strengths under the same conditions.

3-Phenyl-*N*,*N*-dimethylpropylamine[20] was prepared from 3-phenylpropylamine (Aldrich). This material (5 g) was refluxed overnight with 20 mL of formic acid plus 20 mL of aqueous formaldehyde (excess). Following an aqueous workup, the product was distilled at 160 °C (30 mm) and characterized by ^1H NMR and mass spectrometry. The samples examined in this study were 98.6% pure by gas chromatographic analysis (2 m × 3 mm OV-17 on Chrom G, 200 °C). As an internal purity check, the EI mass spectra of P3NM as well as that of the other molecules is shown in Figure 3. The relative ionic signal strengths of the important P3NM peaks are reported for the first time in Table I.

Background pressures were $<3 \times 10^{-7}$ torr in the ionization region and $<7 \times 10^{-8}$ torr in the flight tube. Gas pressures were typically $0.3–5.0 \times 10^{-5}$ torr in the ionization region. (All pressures reported were measured with a Bayard–Alpert ionization gauge, and are uncorrected for the differing sensitivity to the compounds used.) To ensure statistical reproducibility, data were averaged for 500 or 1000 laser shots, depending on the signal strength. TMA and P3NM were introduced through the LTOFMS molecular leak inlet; toluene, through the second "direct" inlet previously described.[1c] The latter was used to achieve higher ionization region pressures and to avoid sample contamination.

Wavelength scans were taken using a stepping motor to drive the dye laser grating at an approximate rate of 200 or 240 s/nm (depending on the laser grating order) with the laser operated at 10 Hz and a fixed laser power. Signals from the CVC's single mass monitor and total output monitor were plotted on chart recorders. Simultaneously, the ion–electron multiplier's anode signal was processed through a Boxcar Averager (PAR) and outputted to a third recorder. This arrangement made it possible to monitor two masses and the total signal simultaneously.

In the region between 415 and 530 nm, the laser dyes stilbene 420, C460, C480, and C500 (Exciton) were used. Wavelengths in the 372–377-nm range were produced by mixing the dye laser (Kiton Red or R610) output with the Nd:YAG fundamental in a nonlinear optics crystal. Since the KDP crystal used for this had to be manually tuned at each wavelength, continuous wavelength scans were impossible. Instead, mass spectra were taken at fixed-wavelength intervals within the region and constructed into excitation spectra via computer plotting routines. Such spectra are viable since phenyl MPI excitation spectral features are broad in this region.[3] These spectra are less reliable than the continuous scans because of the extreme dependence of the laser beam profile on the exact angle setting of the mixing crystal and input laser beams.

Figure 2 indicates the relative consistency of the data over several dye ranges (delineated by brackets). The figure shows the total ion intensities of P3NM and toluene relative to that of TMA as a function of wavelength. Major features of interest will be discussed in later sections. For

(26) H. M. Rosenstock, K. Draxl, D. W. Steiner, and J. T. Herron, "Energetics of Gaseous Ions", *J. Phys. Chem. Ref. Data*, **6**, Suppl. No. 1 (1977).

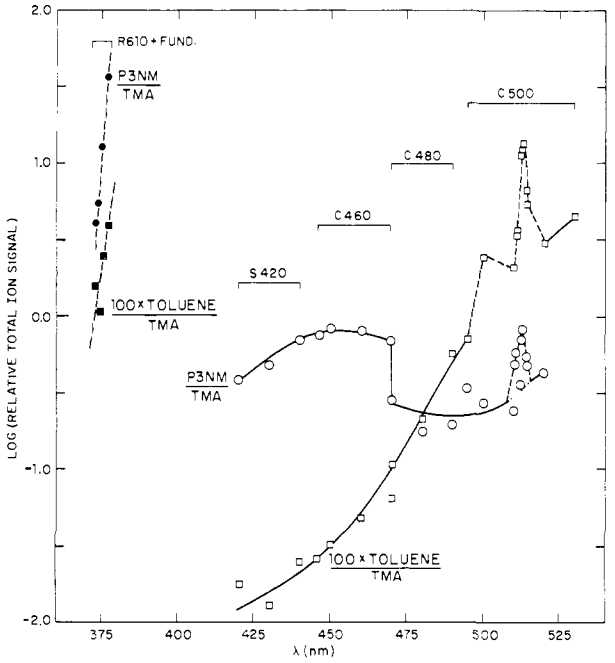

Figure 2. Semilog plot of ion intensities for P3NM (○) and toluene (□) relative to that of TMA excitation vs. wavelength. Ratios are obtained from the individual pure compounds, run within 2 days and scaled to the same sample pressure and instrumental settings. The laser power was 5.0 mJ per pulse, focused through a 0.25-m focal length (f.l.) lens, except for the filled data points, which were at 2.0 mJ per pulse, focused through a 0.50-m f.l. lens (see Experimental Section). The discontinuity at 470 nm is attributed to difficulty in matching laser characteristics at the boundaries of the dye regions. Note that a plot of P3NM/(TMA + toluene) would be essentially identical with that of P3NM/TMA shown.

each dye, the ion intensities were measured at several laser powers; the data presented in Figure 2 were selected from experiments carried out at a single laser power over the entire wavelength range. As a consequence of avoiding saturation of the initial two-photon transition while maintaining a significant signal, it was never possible to have the same laser power and focusing conditions for the full wavelength range (370–530 nm). Thus, in Figure 2 and subsequent figures, there is, effectively, an alteration at 400 nm.

Mass fragmentation patterns in this paper are presented in bargraph form. The heights of the bars represent the area under each mass peak. The total signal from $^1/_2$ amu below to $^1/_2$ amu above a mass is summed, and that sum is given as the signal for that mass. The best general estimate of the error in bar heights is 2% of the largest peak in the region (the portion of the plot under the same magnification).

Results

The LTOFMS system was used to characterize the REMPI fragmentation of the P3NM molecule in the regions from 372.4 to 377.2 nm and from 415 to 530 nm. Data were collected under essentially identical conditions for toluene and trimethylamine (TMA) to document the behavior of the individual chromophores.

To guarantee the identity and purity of all samples, and to verify the proper operation of the mass spectrometer, conventional electron ionization (EI) spectra were taken in the apparatus before the laser was turned on. While most of the data will be presented in bargraph form, the actual resolution of the apparatus was always greater than 200 amu.

Typical 70-eV EI spectra of the three molecules are shown in Figure 3. The fragmentation patterns for toluene and TMA are in good agreement with the literature.[27] The room-temperature gas-phase 70-eV EI fragmentation pattern for P3NM is listed in Table I, which also identifies the species most probably responsible for various m/z values. As in the case of the EI[27] (and MPI[7]) spectrum of triethylamine (TEA), the primary ionic fragmentation product is formed by cleavage of the bond adjacent to the α carbon

(27) "Atlas of Mass Spectral Data", E. Stenhagen, S. Abrahamsson, and F. W. McLafferty, Eds., Wiley-Interscience, New York, 1969.

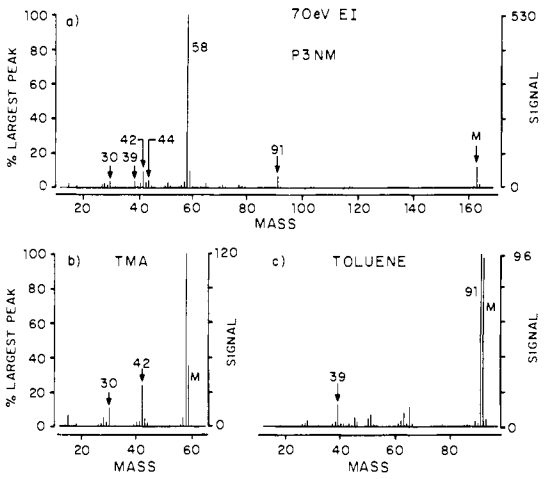

Figure 3. Electron impact mass spectra (70 eV) with intensities scaled to 1.0×10^{-5} torr: (a) P3NM (taken at 3.6×10^{-6} torr); (b) TMA (3.2×10^{-6} torr); (c) toluene (2.6×10^{-6} torr). Note that the intensity of peak m/z 42 is larger than that of m/z 44 in P3NM; note also the high degree of fragmentation of TMA. The right-hand scale on this and subsequent mass spectra denotes relative intensities for one spectrum vs. others in the same figure.

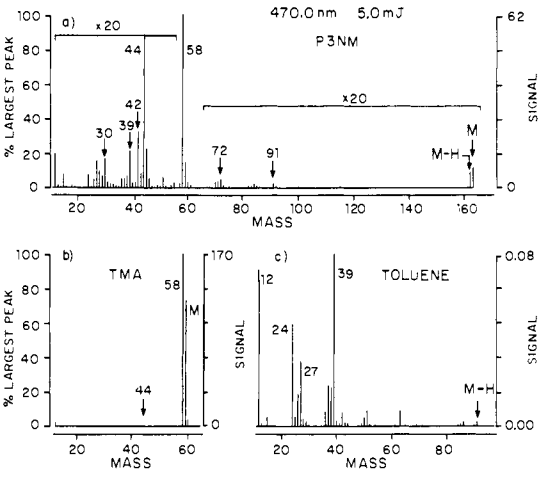

Figure 4. MPI mass spectra at 470.0 nm and 5.0 mJ per pulse (using a 0.25-m f.l. lens) scaled, for comparison, to 1.0×10^{-5} torr: (a) P3NM (taken at 3.0×10^{-5} torr); (b) TMA (3.0×10^{-6} torr); (c) toluene (5.7×10^{-6} torr). Note that the m/z 44 signal is larger than that of m/z 42 in P3NM; cf. Figure 3. Note also the lack of fragmentation in TMA and the low $M^{+\cdot}$ intensity in toluene.

on the amino group, yielding m/z 58 for P3NM. The corresponding fracture at the benzylic position of the molecule produces the less prevalent m/z 91 ion.

Representative MPI fragmentation spectra of the three molecules are shown in Figure 4. The results shown in Figure 4 were obtained at 470.0 nm and (as is the case with most of the data presented) at 5.0 mJ/pulse, focused by a 0.25-m focal length lens. One expects the fragmentation pattern for each molecule to be a function of both the excitation wavelength and the laser beam flux. While many aspects of the spectra do change as one varies these parameters, certain key features are constant. Comparison of Figure 4a with Figures 4b and 4c indicates that the fragmentation behavior of the P3NM is dominated by bond cleavage typical of an amine, mass 58 being the dominant peak. While contributions from masses 12, 24, 27, and 39 are present, their intensities are much lower than that expected from phenyl ring fragmentation in simple alkyl benzenes. A list of observed fragments of P3NM and their typical strengths using multiphoton ionization at several laser powers and wavelengths is given in Table II.

Figures 5, 6, and 7 indicate the laser power dependence of the fragmentation for toluene, TMA, and P3NM, respectively. These

Table II. Observed Fragments from P3NM under MPI,[a] $420 \lesssim \lambda \lesssim 530$ nm

m/e[b]	assignment	rel intensity[c]
12	$C^+\cdot$	w–m
15	CH_3^+ $(NH^+\cdot)^R$	w
18	C_3^{2+} ?	vw
24	C_2^+	w
27^R	$C_2H_3^+$ or $HCN^+\cdot$	m–w
30^R	$C_2H_6^+$ or CH_4N^+	m–w
39	$C_3H_3^+$	m
42	$C_2H_4N^+$	m
44	$C_2H_6N^+$	m
58^d	$CH_2N(CH_3)_2^+$	s–vs
72	$C_4H_{10}N^+$	vw–w
91^e	$C_7H_7^+$	vw
162	$[M-H]^+$	w
163^M	$C_6H_5(CH_2)_3N(CH_3)_2^{+}\cdot$	w–s

[a] Typical for data taken under conditions where quadratic laser power dependence was observed. [b] M = molecular ions, R = rearrangement product. [c] v = very, s = strong, m = medium, w = weak. [d] Cleavage of 1,2 bond, α to amino group. [e] Cleavage of 1,2 bond, α to phenyl group.

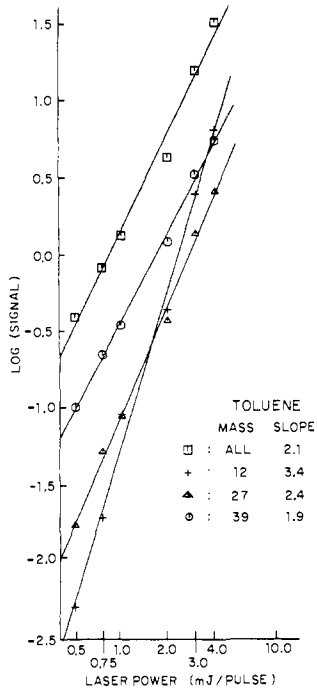

Figure 5. Log–log plot of laser power dependence of toluene at 372.85 nm, using a 0.50-m f.l. lens, taken at 3.0×10^{-5} torr, but scaled to 1.0×10^{-5} torr. Data presented for the total signal detected (□), and masses 12 (+), 27 (△), and 39 (○). Slopes determined using least-squares linear regression fit (±0.2).

figures show that as the laser flux is changed the P3NM response also resembles that of an acyclic amine.

The laser power dependence of the toluene (Figure 5) is very similar to that of benzene,[13] and typical of benzenoid structures. The total signal (□) is approximately quadratic, as is expected when the initial ionization process is rate limited by a two-photon absorption. Individual fragments tend to have increasingly higher order laser power dependence (39 < 27 < 12) as the total number of photons needed to form the given product increases. Thus, as the laser power increases, the fragmentation pattern becomes dominated by lower mass ions. The laser power dependence does not change significantly with wavelength between 370 and 520 nm. Data from 372.8 nm are presented as the toluene signal strength (and S/N) is large at that wavelength.

The series of partial TMA spectra (Figure 6) shows only the main ion peaks, at a wavelength where the two major fragmentation components (molecular ion at mass 59 and $[M-H]^+$ at 58) are of nearly equal signal level. The series of mass spectra

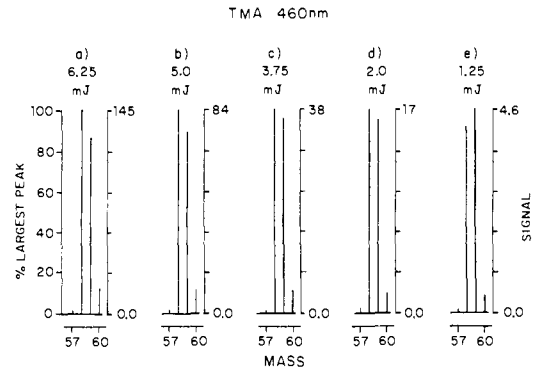

Figure 6. TMA fragmentation at 460.0 nm at various powers, using a 0.25-m f.l. lens. Signals at lower masses were extremely small (cf. Figure 4b) and are not shown in this plot. These data were taken at 3.0×10^{-6} torr, but signal intensity has been scaled to 1.0×10^{-5} torr. Note that, contrary to ref 7, there is a slight power dependence to the fragmentation. Signal at m/z 60 above the isotopic level is spurious, caused by slow multiplier recovery.

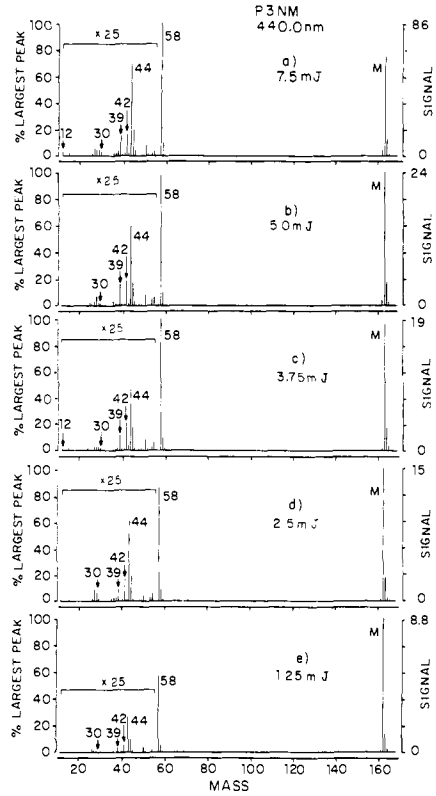

Figure 7. P3NM fragmentation at 440.0 nm at various laser powers, using a 0.50-m f.l. lens, taken at 1.0×10^{-5} torr. Note that ion intensities for m/z <57 are multiplied by a factor of 25 and also that the ratio of m/z 58 to m/z 163 increases with laser power.

presented are actually atypical of tertiary amines. At most wavelengths, either molecular ion or $[M-H]^+$ is heavily dominant and the fragmentation pattern is independent of laser power, typical behavior for uncaged amines.[7] The power dependence (intensity inversion) seen in Figure 6 is found only when competition exists between processes giving rise to the different ions. Thus, in Figure 6 at 460.0 nm, three photons are just sufficient to ionize the molecule, producing m/z 59; if any relaxation takes place prior to ionization, a fourth photon is necessary, exciting the molecule well above threshhold for m/z 58 production. This laser power dependence is a very weak effect. If these data were plotted as in Figure 5, two parallel lines would result, since, both ions 58 and 59 have the same power dependence (2.1 ± 0.1) and since this wavelength shows the largest power dependence seen for TMA fragmentation, it is clear that TMA and toluene are very different in their fragmentation power dependences.

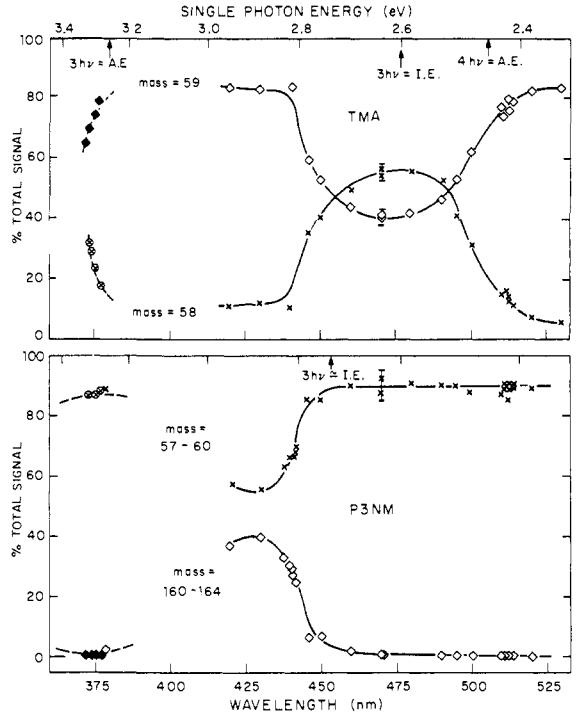

Figure 8. Percent molecular (◇) and principal fragment (×) ions vs. wavelength for TMA (top) and P3NM (bottom). All data are at 5.0 mJ per pulse using a 0.25-m f.l. lens except in the 375-nm region (circled data points for daughter ions; filled data points for molecular ions) where 2.0 mJ per pulse and a 0.50-m f.l. lens were used. For TMA, molecular ion is mass 59 and fragment mass 58, while for P3NM, molecular ion was taken as masses 160 through 164, principle fragment as masses 57–60. The lowest appearance energy (AE) is shown for TMA, but not for P3NM where data were insufficient for a reliable determination. P3NM fragment fractions invert under some focusing conditions.

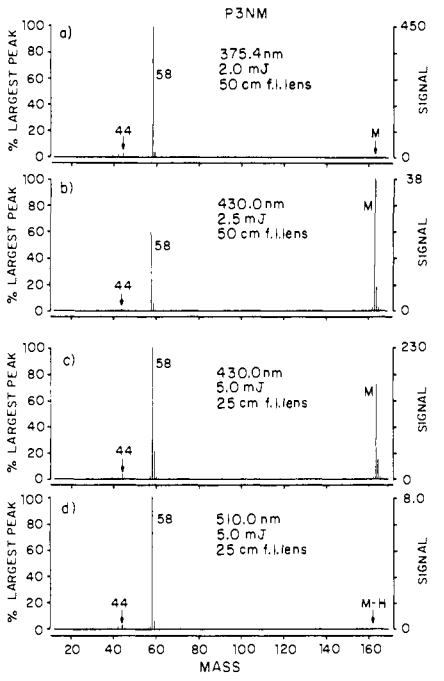

Figure 9. P3NM mass spectra, showing the wavelength dependence of the fragmentation. (a) and (d) were taken at 3.0×10^{-6} torr, (b) and (c) at 1.0×10^{-5} torr. All spectra were scaled to 1.0×10^{-5} torr. Note the varying laser wavelength, power, and focusing conditions listed on each spectrum.

P3NM, as shown in Figure 7, is similar to TMA. Here conditions (wavelength and focusing lens) were chosen for which the two major fragments (mass 58 and the molecular ion) are again approximately equal. This equivalence occurs at a different wavelength (440.0 nm) than it does for TMA. Again a power dependence difference between the molecular ion and mass 58 is apparent. Although the total ion signal is quadratic (1.8 ± 0.2), the ion signals from individual masses differ greatly in laser power dependence. This behavior is, however, atypical for P3NM. As in TMA, the series of mass spectra presented demonstrates the largest deviation seen from uniform quadratic power dependence in P3NM. At virtually all wavelengths, there is almost no increase in the fraction of small fragments (<58 amu) relative to that of mass 58, or in the low mass fragmentation pattern as laser power varies. Such shifts would be expected if phenyl fragmentation were a major channel. Figures 6 and 7 contain spectra for the wavelengths which show the greatest fragmentation laser power dependence for TMA and P3NM, respectively. They indicate upper bounds for this effect. At most wavelengths, the fragmentation pattern is relatively independent of laser power for both molecules.

Another similarity between P3NM and TMA is in the variation of the mass 58 and the molecular ion as a function of wavelength, as shown in Figure 8. In certain wavelength regions mass 58 is overwhelmingly dominant, amounting to more than 80% of the total signal detected. At other wavelengths (between 410 and 444 nm for P3NM), the molecular ion is a major component. The new result for TMA, shown in Figure 8a, is almost identical with that of ref 7. The variation of the relative intensities of the two P3NM peaks is displayed in Figure 9, which shows the MPI fragmentation pattern of the molecule at several wavelengths and laser powers. While the behavior of P3NM does in this respect mimic that of uncaged tertiary amines (both TMA and TEA[7]), there is also an important difference. In the case of P3NM, conditions could never be found in which the molecular ion contribution to the total signal was greater than 60%, whereas for TMA and TEA (which lose H and CH_3, respectively) values >95% have been observed.

Table III. Total Ion Intensities of Toluene and P3NM Relative to TMA[a]

λ (nm)	toluene	P3NM
375.4[b]	3×10^{-2}	13
420.0	2×10^{-4}	0.4
460.0	5×10^{-4}	0.8
510	2×10^{-2}	0.3
512.4[c]	1×10^{-1}	0.7 ± 0.3
520	3×10^{-2}	0.4

[a] Summary of data presented in Figure 2. Values scaled to TMA = 1 at each wavelength. Data taken at 5 mJ/pulse with 0.25-m focal length lens, unless otherwise noted. [b] 2 mJ/pulse with 0.50-nm focal length lens. [c] ^1L_b 14^1_0 transition of toluene.

The ratio of ion intensities of mass 163 (molecular ion, $M^{+\cdot}$) to mass 162 ($[M - H]^+$) also changes with wavelength: below 470 nm mass 163 ($M^{+\cdot}$) is by far the larger peak. At longer wavelengths where the total signal carried by ions of $m/z > 160$ is very weak, the $[M - H]^+$ ion is the more intense. For this reason what is plotted in Figure 8 as P3NM "molecular ion" is the group of masses having the structural skeleton of P3NM regardless of the number of hydrogens (chiefly m/z 162 and 163). The implications of this hydrogen loss will be examined in the Discussion section.

Finally, as shown in Figure 2, and summarized in Table III, the total ion signal from P3NM is of the same order of magnitude as that of TMA. This is to be compared with the total toluene signal which is some three orders of magnitude lower than TMA and P3NM. It should be noted that at all wavelengths greater than 400 nm the P3NM signal is slightly smaller than that of TMA at comparable pressures (i.e., 20 to 80%), but it can be considerably higher at shorter wavelengths.

In order to establish the role of the phenyl ring in the fragmentation process of P3NM, a comparison was made of the relative proportion of mass 39 ($C_3H_3^+$) to total signal. Mass 39 is used here as a tracer of phenyl group fragmentation. This choice was made for three reasons. First, m/z 39 is a known major fragment from phenyl ring MPI fragmentation.[8c] Second, frag-

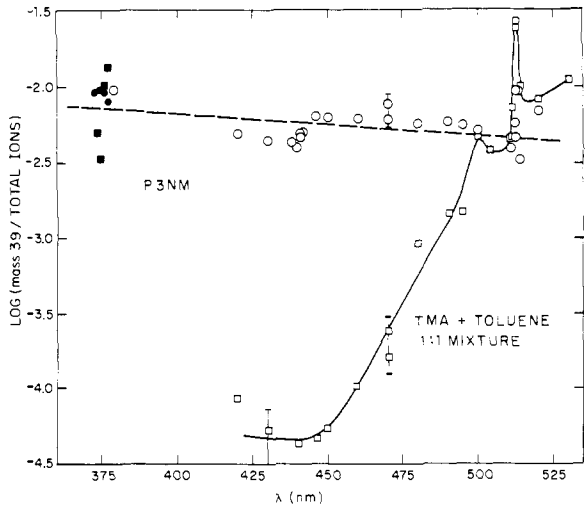

Figure 10. Log plot of fraction of total ion current due to m/z 39 vs. wavelength for P3NM (○) and a 1:1 TMA to toluene mixture (□). Peak near 510 nm is significant; see text for commentary on these data. Data were obtained using 5.0 mJ per pulse with a 0.25-m f.l. lens, except filled data points, which were taken at 2.0 mJ per pulse with a 0.50-m f.l. lens. Note comparison with Figure 2.

mentation of the amine moeity should not give rise to m/z 39 unless the neutral fragments were subsequently ionized. But if secondary ionization were taking place, the total ion signal laser power dependence would not be quadratic, since one (two-photon) excitation gives rise to more than one ion. The chance of the m/z 39 ion originating in the three-carbon alkyl chain is very small. Alkyl chains do generate ions of mass 39, but they are always accompanied by more intense signals at masses 41, 42, and 43.[27] Although EI and MPI fragmentation results are not necessarily equivalent, the lack of m/z 40 and 41 at all wavelengths suggests that m/z 39 originates in the fragmentation of the phenyl ring. Third, P3NM mass spectra were obtained in sections, one of which was $m/z < 58$. Since m/z 39 is a large fragment in this region, the mass 39 ion signal is accurately determined despite the fact it comprised less than 1% of the total ionic signal. Figure 10 compares the percentage of mass 39 in P3NM to that in a hypothetical 1:1 mixture of the isolated chromophores (i.e., toluene and TMA).[28] As expected, the percent of 39 (%39) in the signal from a 1:1 mixture of TMA and toluene is dependent on the total signal from the individual components of the mixture. Therefore, between 400 and 470 nm where the total toluene signal is very small relative to TMA (see Table III), the %39 in a 1:1 mixture is very low. As one can see in the upper curve of Figure 10, the %39 from P3NM is relatively constant, increasing slightly with decreasing λ. This result is indicative of internal energy redistribution before fragmentation.

A second method used to detect influences of the phenyl group on MPI fragmentation was to scan the laser excitation wavelength through known resonances of toluene. Two regions were studied: 373–382 nm, corresponding to the transition to the 3p Rydberg state of toluene,[3] and 480–530 nm, corresponding to the ^1L_b ($^1B_2$) state.[12]

The transition to the 3p Rydberg state of toluene has been investigated by Uneberg et al.,[3] who found the two-photon origin to be at 378.5 nm. At shorter wavelengths they show a continuing, but decreased, signal. In the present experiments with toluene, the total ion current increased as the wavelength was scanned toward the UV. Since a larger signal would make it easier to observe a phenyl contribution to the total P3NM signal, considerable effort was spent investigating the 373- to 378-nm region of the P3NM MPI spectrum. Unfortunately, owing to operating conditions discussed in the Experimental Section, the excitation spectra were of poor quality. Only data which were consistently reproducible (e.g., %39) from this wavelength region are reported.

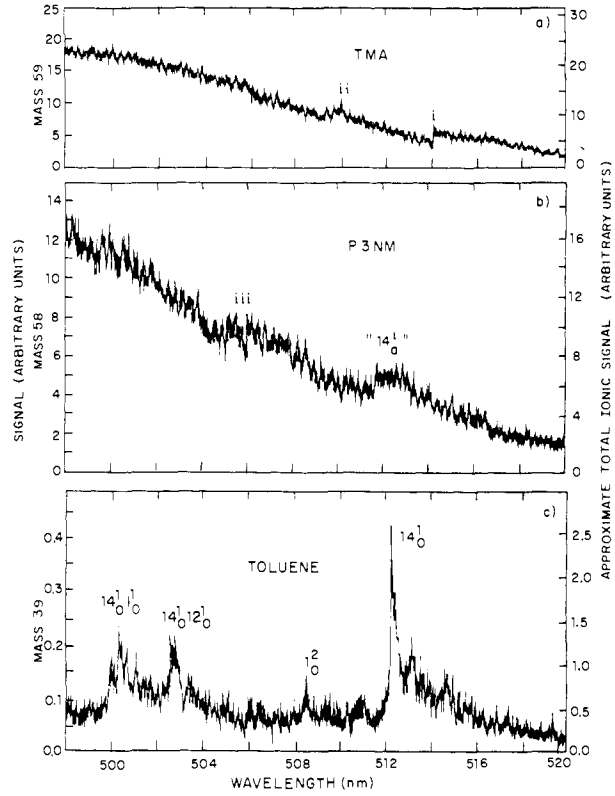

Figure 11. Excitation spectra of (a) TMA (taken at 6.0×10^{-6} torr), (b) P3NM (6.0×10^{-6} torr), and (c) toluene (5.0×10^{-5} torr) between 498 and 520 nm. All scans were taken at 10 mJ per pulse with 0.25-m f.l. lens. Intensity axis scales have been scaled to 1.0×10^{-5} torr, and compensated for all known variations in electrometer gain. The features in the TMA spectrum, the "hump" at 509.5 nm labeled (i) and the shift at 514 nm labeled (ii), are known artifacts. The main resonance lines in the toluene spectrum have been identified. The left-hand axis of each spectrum is the intensity of the monitored ion. The right-hand axis is determined by dividing the detected signal by the fraction of the total molecular signal represented by the monitored ion. For TMA, the fraction represented by m/z 59 changes with λ, and the average fraction is used. For P3NM, there is a small change in the fragmentation at 512.4 nm but the approximation for total molecular signal remains adequate. Note the P3NM feature labeled "14_0^1" at ca. 512.4 nm, which is discussed in the text, and that labeled (iii), which, while reproducible, has not been assigned.

MPI spectroscopy of the ^1L_b state of substituted benzenes has been thoroughly investigated by Goodman's group.[12] The most intense peak is found to be the 14_0^1 transition at 512.2 nm. (This peak is reported here as being at 512.4 nm, the location of its maximum in our excitation spectra.) While the toluene signals, even at the resonance peak, are much lower than those obtained in the 375-nm region, certain features make the 495–530-nm region favorable for examining phenyl-derived signals in P3NM. First, the dye laser scans are stable; second, TMA signals are particularly weak in this region; and third, the ^1L_b transition is well structured in this region. The last of these factors should produce readily identifiable features in the P3NM excitation spectrum. These features are superimposed on a monotonically decreasing (with increasing wavelength) amine contribution. Indeed, as seen in the P3NM excitation spectrum, Figure 11b, one does find such a "hump" at ca. 512.4 nm, readily reproducible, which is identified with the strong 14_0^1 transition in toluene. A similar structure can be seen at 512.4 nm in the ion intensity plot in Figure 2. Excitation spectra of TMA and toluene are also shown in Figure 11 for comparison. [The sharp step function rise,

(28) (a) Attempts were also made to run mixtures of TMA and toluene in the LTOFMS. Because of the extremely large difference in total MPI signal strength from these two molecules, it was necessary to use a very small fraction (e.g., 5%,) of TMA in such mixtures. Minimal fluctuation in the TMA pressure, which could not be monitored under these conditions, became a major source of error. Therefore, data from separate experiments on the individual molecules, identical except for sample pressure, were combined after scaling all results to 1.0×10^{-5} torr. (b) F. P. Lossing, *Can. J. Chem.*, **49**, 357 (1971); (c) F. A. Elder and A. C. Parr, *J. Chem. Phys.*, **50**, 1027 (1969).

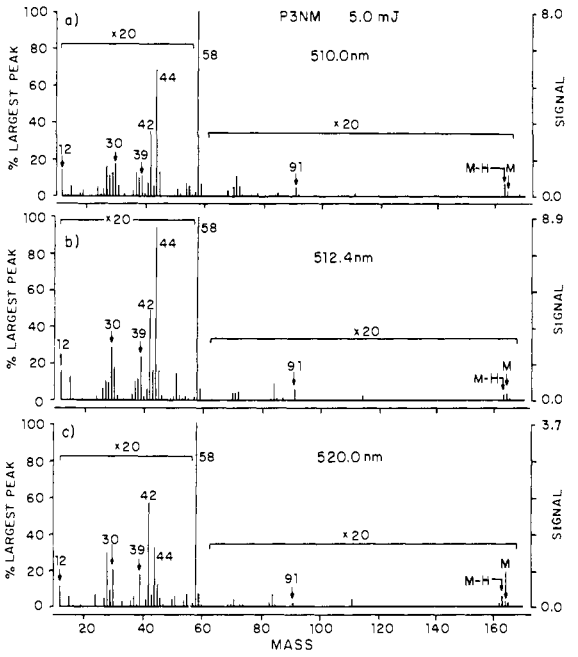

Figure 12. P3NM mass spectra at (a) 510.0 nm, (b) 512.4 nm, and (c) 520.0 nm, 5.0 mJ per pulse using a 0.25-m f.l. lens, taken at 3.0×10^{-6} torr, but intensities scaled to 1.0×10^{-5} torr, showing the fragmentation behavior spanning the phenyl resonance at 512.4 nm. The anomalous behavior of m/z 42 at 520.0 nm is not understood.

labeled i, in the TMA spectrum at 514.0 nm is due to an uncalibrated increase in gain after a momentary interruption of the experiment, while the "hump" labeled ii in that spectrum, at ca. 509.5 nm, is due to a pressure adjustment; both features are spurious.]

The effect of the 512.4-nm feature in the P3NM excitation spectrum on the mass fragmentation pattern is displayed in Figure 12. It is seen that there is an increase in the relative level of all (not just phenyl-derived) low mass components (<58 amu) at the phenyl resonance wavelength. There is also an increase in total signal at the resonance. This increase of approximately 40% (measured by total ionic signal) is near that expected if the phenyl resonance contribution were additive. From Figure 11 one can also observe in P3NM a ca. 30% increase in the m/z 58 ion at the 512.4-nm resonance peak.

Discussion

(i) The Amine-Like Behavior of P3NM. The MPI excitation spectrum and the MPI fragmentation pattern of the 3-phenyl-1-(N,N-dimethylamino)propane bichomophore (P3NM) are predominately those of an amine. The first of these observations can be simply explained; the signal strength of the isolated amine, TMA, is far greater than that of toluene at all wavelengths investigated, as seen in Table III. The fragmentation pattern, however, contains much more information and will be discussed in detail below. Specifically, the question of whether this molecule's fragmentation is statistical in nature, and the role of intramolecular energy redistribution, will be explored.

Two of the main characteristics of the amine-like fragmentation behavior of P3NM are the prevalence of the ion formed by fracture at the amine's α carbon, and the ratio of this fragment's signal to that of the molecular ion as a function of wavelength. These effects have been previously analyzed for the simple amines, TMA and TEA, in ref 7. The major daughter ion was found to be that with the lowest appearance energy (AE), that ion arising from the breaking of the weakest bond on the α carbon. As the excitation frequency is tuned from a region where four photons are sufficient to produce only the molecular ion to a frequency above the threshold for formation of the least "expensive" daughter ion (i.e., that of lowest AE), the latter ion is found to sharply increase in intensity. As the frequency is further increased, so that the energy of three photons exceeds the ionization energy (IE) (but not by enough to yield fragmentation to daughter ion), this lower order process dominates. The trend toward greater production of daughter ion is thus reversed. By determination of the points of reversal, both the IE of the amine and the AE of the daughter fragment can be found.

Scheme III

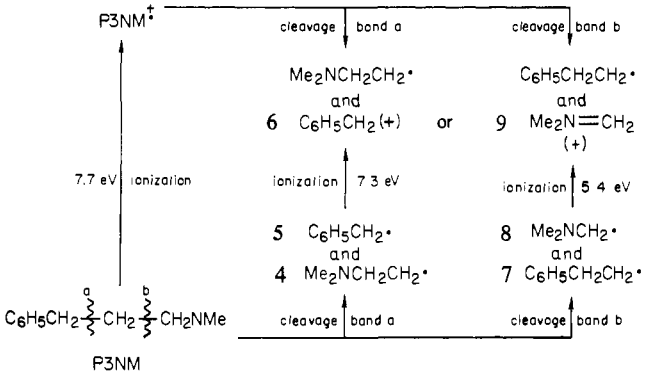

Parker et al.[7] carried out this analysis for TMA and TEA and found values for the ionization energy and the principal daughter ion appearance energy in reasonable agreement with values determined independently. Applying this approach to the data in Figure 8 yields a value of ca. 8.2 eV for the ionization energy of P3NM. This compares with values of 7.8 eV for TMA,[26] 7.5 eV for TEA,[26] and 7.7 eV for P2NM.[22] Loguinov et al. report an appearance energy of 8.2 eV for the m/z 58 ion from P2NM.[22] Analysis of Figure 8 leads to an estimated value of ca. 9.0 eV for the appearance energy of this ion in P3NM, though because of the lack of data between 415 and 380 nm, there is much uncertainty in this value.

(ii) Energetics of the Molecular Ion Fragmentation. One of the problems with this analysis of the MPI excitation spectrum of the m/z 163 and 58 ions for the P3NM is that it presumes that the molecular ion in P3NM is transparent to one-photon absorption in this wavelength region. Light absorption by $M^{+\cdot}$ would lead to the formation of ions of lower mass by an "ionic ladder" climbing process. The $M^{+\cdot}$ population would decrease, accompanied by an increase in the intensity of other ions including m/z 58. The curve shapes in Figure 8 would thereby be distorted, and the values calculated for the IE of P3NM and the AE of the mass 58 would be in error.

There is some indication in Figure 8 that light absorption by $M^{+\cdot}$ does take place. Unlike the simple amines of ref 7, no wavelength could be found where the daughter ion signal in P3NM approaches zero signal. Some light absorption by the molecular ions of P3NM in this wavelength must take place. The molecular ion could not be strongly absorbing or the "amine-like" behavior shown in Figure 8 would not be observed. Scheme II provides an explanation for this apparent dichotomy. The phenyl-centered ion **1** lies approximately 1 eV higher in energy than the amine-centered ion **2**. At the threshold for three-photon ionization of P3NM, a negligible fraction of molecular ions would be in the form **1**. As the excitation pulse is scanned to shorter wavelengths, $M^{+\cdot}$ is produced with a higher internal energy. One anticipates a quasi-thermal distribution among the ions in Scheme II, and ion **1** should be strongly absorbing at these wavelengths.[18] If the molecular ions of P3NM were uniquely "amine-like" (e.g., form **2**), behavior identical with that of ref 7 for TMA and TEA would be observed. If, however, **1** and **2** reached equilibrium on the time scale of the 5-ns laser pulse, subsequent photon absorption by **1** would lead to enhanced molecular ion fragmentation. Its importance would increase at shorter wavelengths. The data in Figure 8 are consistent with this model.

The primary fragmentation of $M^{+\cdot}$ can, in principle, occur by cleavage of either bond a or bond b (Schemes I and III). Sufficient thermochemical data exist for estimating the energy changes associated with these reactions. Bonds a and b are of comparable energies in neutral P3NM. Using known C–H bond strengths in TMA and toluene, and assuming that the β-sub-

stituents in **4** and **7** do not affect the stability of the primary $-CH_2$ radical, one can estimate that cleavage of bond a in the neutral is favored over bond b cleavage by only 0.1 eV. From the ionization energies of $C_6H_5CH_2\cdot$ (7.3 eV)[29] and $Me_2NCH_2\cdot$ (5.4 eV),[22] one sees that the ionization of the latter is strongly favored. Consequently, fragmentation at bond b in the molecular ion of P3NM is energetically favored by ca. 2 eV over that at bond a. If energy considerations alone control the fragmentation pattern of $M^{+\cdot}$, the mass 58 ion ($Me_2NCH_2^+$) should overwhelmingly dominate mass 91 ($C_7H_7^+$) and its associated ions in the MPI fragmentation pattern of P3NM, as observed.

(iii) Energy Redistribution in P3NM. Because of its relatively small contribution to the total signal at most wavelengths, the phenyl chromophore has almost no effect on the P3NM molecule's MPI fragmentation. However, as indicated by the appearance of the 14_0^1 resonance in a region of very low amine signal, the P3NM excitation spectrum does contain a phenyl contribution. It is expected that the excitation of the two parts of the molecule should be independent and additive, and this is seen for the total ion signal in the 498- to 520-nm region (cf. Figure 11). Deviation from this behavior is found at shorter wavelengths and will be discussed below.

An interesting result of this investigation is the subtle change in the fragmentation patterns obtained when the energy is absorbed via the different chromophores. The P3NM MPI mass spectrum is nearly independent of laser power off the phenyl resonance. As mentioned in the *Results* section (see Figure 10), the approximately constant percentage of mass 39 (and other fragments) off resonance, is indicative of intramolecular energy redistribution, from the amine to the phenyl end, before fragmentation. By tuning to the phenyl resonance, however, there is a distinct increase in the fraction of small fragments (m/z <58). The fact that all small fragments, including the dimethylamine derived ions at m/z 42 and 44, i.e., not just those identified with the phenyl ring, are enhanced at the phenyl resonance, again indicates energy redistribution, here from the phenyl to the amine end. This result leads to the conclusion that *energy redistributes out of both the chromophores*. It is not possible, on the basis of these experiments, to determine whether the redistribution is occurring in the neutral or the molecular ion or both.

(iv) Photochemistry and Ion Yield. One of the curious observations in MPI studies of benzene derivatives is the relatively low ion signal produced. Figure 2 shows the magnitude of the effect. What makes the low ion yield from benzene derivatives so unusual is that it occurs in a wavelength region where the one-photon extinction coefficient for the phenyl group is substantially larger than that for amines. What evidence there is suggests that the corresponding two-photon cross section at these wavelengths favors absorption by phenyl over amine since both transitions are of g → u origin. One expects, therefore, that two-photon excitation of benzene and its derivatives would produce a higher concentration of low-energy singlet states than would excitation of simple amines.

In striking contrast, P3NM yields only slightly less ion current than TMA for excitation in the region 420–520 nm, and *substantially* more ion current for excitation into the B band of toluene at 375–380 nm. Since this band is of g → g origin (in benzene), it is an allowed two-photon transition. One notes in Figure 2 that ion formation in toluene is enhanced at these wavelengths. It remains significantly less than that for TMA.

A literature search suggested that rapid photochemical rearrangement reactions in alkylbenzenes might be responsible for these low ion yields. For example, benzene molecules, excited to their second or third singlet states, have been shown to lose energy by highly efficient nonradiative processes.[30] These processes become more important at shorter wavelengths and lower pressures in the vapor phase. For example, benzene vapor, excited at 184.9 nm, shows virtually no fluorescence. Other results, in combination with this observation, point to quantum yields near unity for benzene disappearance when low-pressure benzene vapor is irradiated at this wavelength.[31] The major product of benzene

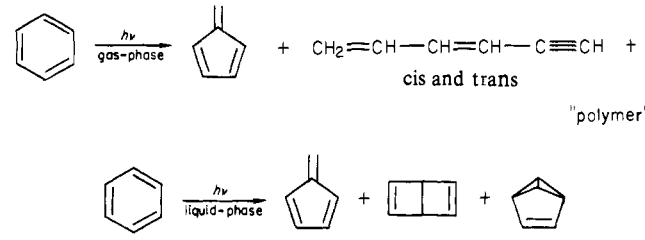

disappearance is a polymeric material. This may be the same material that certain research groups studying the MPI behavior of benzene and its derivatives find coating the optics of their apparatus.[3] Its structure and immediate precursors are unknown. Since irradiation of benzene in the liquid phase forms Dewar benzene and benzvalene in addition to fulvene,[30] vibrationally excited forms of these molecules or their thermal rearrangement products might be the precursors of the polymeric material observed. These reactions also occur with alkyl-substituted benzenes.

This evidence suggests that one reason for the relatively low ionic signals observed in MPI studies of benzene and its derivatives (relative to that of the amine) is the rapid occurrence of photochemical reactions yielding neutral species. If the products are transparent to one-photon excitation at wavelengths longer than 370 nm, then their formation would compete with further excitation of alkylbenzene excited states.

The high ion yield of P3NM for two-photon excitation at 370 nm is thus particularly noteworthy. As shown in Table III and Figure 2, the ionic signal of P3NM is one order of magnitude greater than TMA and three orders of magnitude greater than toluene. In this wavelength region the two-photon absorption cross section of the phenyl group should be significant. It is possible that the presence of the amino group in P3NM quenches the photochemical reactions of the phenyl group. This might occur by rapid crossing to a charge-transfer state of the neutral molecule. The latter state must persist long enough to absorb photons in the 370–400-nm range during the 5-ns laser pulse. Thus ion formation could be substantially enhanced over that in toluene. The results of the excitation at 512.4 nm would indicate that no CT state exists at ca. 5 eV.

A more thorough investigation of this region at ca. 6.6 eV, where charge-transfer states are expected to exist, should yield important new gas-phase data on these states.

Acknowledgment. The authors appreciate valuable discussions with Professor K. B. Eisenthal and Dr. M. P. Barbalas. This work received financial support from NSF Grants CHE 78-25187 and CHE 81-16368 (D.A.L., D.W.S., and R.B.B.) and NSERC Canada A6 429 (M.A.W.).

Registry No. 3-Phenyl-1-(dimethylamino)propane, 1199-99-1; toluene, 108-88-3; trimethylamine, 75-50-3.

(29) G. Kaupp, *Angew. Chem., Int. Ed. Engl.*, **19**, 243 (1980).

(30) H. R. Ward and J. S. Wishnok, *J. Am. Chem. Soc.*, **90**, 5353 (1968).

(31) L. Kaplan, S. P. Walch, and K. E. Wilzbach, *J. Am. Chem. Soc.*, **90**, 5646 (1968).